Ecological impacts of a widespread frost event following early spring leaf-out

KOEN HUFKENS*, MARK A. FRIEDL*, TREVOR F. KEENAN†, OLIVER SONNENTAG†‡, AMEY BAILEY§, JOHN O'KEEFE¶ and ANDREW D. RICHARDSON†

*Department of Geography and Environment, Boston University, Boston, MA USA, †Department of Organismic and Evolutionary Biology, Harvard University, Cambridge, MA USA, ‡Département de Géographie, Université de Montréal, Montreal, Canada, §USDA Forest Service, Northeastern Research Station, Hubbard Brook Experimental Forest, Campton, NH USA, ¶Harvard Forest, Petersham, MA USA

Abstract

In the spring of 2010, temperatures averaged ~3 °C above the long-term mean (March–May) across the northeastern United States. However, in mid-to-late spring, much of this region experienced a severe frost event. The spring of 2010 therefore provides a case study on how future spring temperature extremes may affect northeastern forest ecosystems. We assessed the response of three northern hardwood tree species (sugar maple, American beech, yellow birch) to these anomalous temperature patterns using several different data sources and addressed four main questions: (1) Along an elevational gradient, how was each species affected by the late spring frost? (2) How did differences in phenological growth strategy influence their response? (3) How did the late spring frost affect ecosystem productivity within the study domain? (4) What are the potential long-term impacts of spring frost events on forest community ecology? Our results show that all species exhibited early leaf development triggered by the warm spring. However, yellow birch and American beech have more conservative growth strategies and were largely unaffected by the late spring frost. In contrast, sugar maples responded strongly to warmer temperatures and experienced widespread frost damage that resulted in leaf loss and delayed canopy development. Late spring frost events may therefore provide a competitive advantage for yellow birch and American beech at the expense of sugar maple. Results from satellite remote sensing confirm that frost damage was widespread throughout the region at higher elevations (>500 m). The frost event is estimated to have reduced gross ecosystem productivity by 70–153 g C m^{-2}, or 7–14% of the annual gross productivity (1061 ± 82 g C m^{-2}) across 8753 km^2 of high-elevation forest. We conclude that frost events following leaf out, which are expected to become more common with climate change, may influence both forest composition and ecosystem productivity.

Keywords: carbon balance, elevational gradient, frost event, northern hardwood forest, phenology

Received 5 December 2011; revised version received 23 March 2012 and accepted 25 March 2012

Vegetation phenology in temperate ecosystems is strongly linked to seasonality in photoperiod and temperature (Schwartz *et al.*, 2006). As a result, observed changes in phenology have been widely linked to climate change processes, and current estimates suggest that spring phenology has advanced by as much as 2 days per decade over the last half-century (Parmesan & Yohe, 2003; Jeong *et al.*, 2011). From a community ecology perspective, species-specific phenological events also influence species distributions and community dynamics (e.g. Chuine, 2010). Consequently, changes in phenology have altered species distributions at both geographic (Hickling *et al.*, 2006; Morin *et al.*, 2008) and elevation range margins (Beckage *et al.*, 2008; Lenoir *et al.*, 2008). Indeed, some studies have suggested that

increased spring temperatures in the northern hemisphere will selectively alter species ranges, displacing the range of some vegetation types north by as much as 250 km (Iverson & Prasad, 1998). Other recent studies have reported changes in the elevation range of selected species in southern California, USA (Kelly & Goulden, 2008), western Europe (Lenoir *et al.*, 2008), and the Green Mountains of Vermont, USA (Beckage *et al.*, 2008).

Phenology is also a first-order control on ecosystem carbon cycling (Piao *et al.*, 2009; Richardson *et al.*, 2010). For example, recent changes in the growing season length of North American temperate deciduous forests has increased ecosystem productivity by 10 g C m^{-2} yr^{-1} over the last 10 years (Dragoni *et al.*, 2011). In addition to affecting the carbon cycle, phenology alters atmospheric boundary layer properties, biosphere-atmosphere interactions, and more generally, the biophysical environment of terrestrial ecosystems

Correspondence: Koen Hufkens, tel. + 1 617 353 8846, fax + 32 9 264 6242 , e-mail: koen.hufkens@gmail.com

(Sakai *et al.*, 1997; Hollinger *et al.*, 1999; Fitzjarrald & Acevedo, 2001; Levis & Bonan, 2004). Understanding how phenology responds to climate variability, climate change, and extreme events is therefore essential for improving understanding of how coupled climate-ecosystem dynamics will evolve in the coming decades.

Climate change is expected to increase the frequency of extreme weather events (Solomon *et al.*, 2007; Marino *et al.*, 2011). Specifically, and as a by-product of warmer temperatures, the occurrence of frost after leaf out is projected to become more common in some parts of the world (Meehl *et al.*, 2000; Gu *et al.*, 2008). This scenario has a number of important ecological implications. In particular, newly developed leaves are sensitive to frost events, as they lack the structural rigor necessary to prevent damage. Depending on the timing of spring warmth, early and accelerated leaf development has the potential to increase the frequency and magnitude of leaf damage from freezing events (Norby *et al.*, 2003; Inouye, 2008), and lasting effects may include loss of stored carbon and nutrients, and reduced photosynthetic carbon gain (Gu *et al.*, 2008; Martin *et al.*, 2010).

Global land surface temperatures in 2010 were among the warmest of the last 131 years (Blunden *et al.*, 2011). In the northeastern United States, extraordinarily warm winter and spring temperatures were recorded, averaging 3 °C above the 1971–2000 climatological average for May and June (Blunden *et al.*, 2011; Guirguis *et al.*, 2011). During this period, however, the northeastern United States experienced a late spring freezing event from May 9 to 11 [day of year (DOY) 129–131]. The effects of this event were widespread, and ranged from mild leaf damage to complete defoliation of the canopy (e.g. Fig. 1a and b). As stand level warming and freezing experiments in forest ecosystems are difficult to implement, the co-occurrence of an unusually warm spring with a pronounced late spring frost presents a rare opportunity to study the nature and magnitude of ecosystem responses to climate change and extreme events, and to assess species specific impacts of extreme weather conditions on canopy development.

In this article, we examine the response of sugar maple (*Acer saccharum*), American beech (*Fagus grandifolia*), and yellow birch (*Betula alleghaniensis*) to the anomalous spring of 2010 in the northeastern United States. These three species are widespread in northern hardwood forests (Foster, 1992) and therefore provide a good basis for understanding how northeastern forests respond to climate change and extreme events. We use the unique conditions provided by an unusually warm early spring and late spring frost in 2010, in combination with several different data sources including field observations of vegetation phenology,

Fig. 1 (a) Frost damage to developing sugar maple leaves and (b) landscape view of frost damage 15 days after the event showing damaged sugar maple trees are interspersed with healthy developing American Beech and yellow birch. Photos supplied by Amey Bailey and Paul Schaberg.

eddy covariance measurements, and near-surface and satellite remote sensing imagery to address the following questions: (1) How did each species respond to differences in the intensity of the anomalous spring warmth and frost at different elevations? (2) How do differences in phenological growth strategy influence this response? (3) How did the late spring frost affect ecosystem productivity in northern hardwood forests within the study domain? (4) What are the potential long term impacts of more frequent spring frost events on temperate hardwood forest community ecology?

Materials and methods

Study area and measurement sites

The study area encompasses the northeastern United States covering all of Pennsylvania, Vermont, New York, New
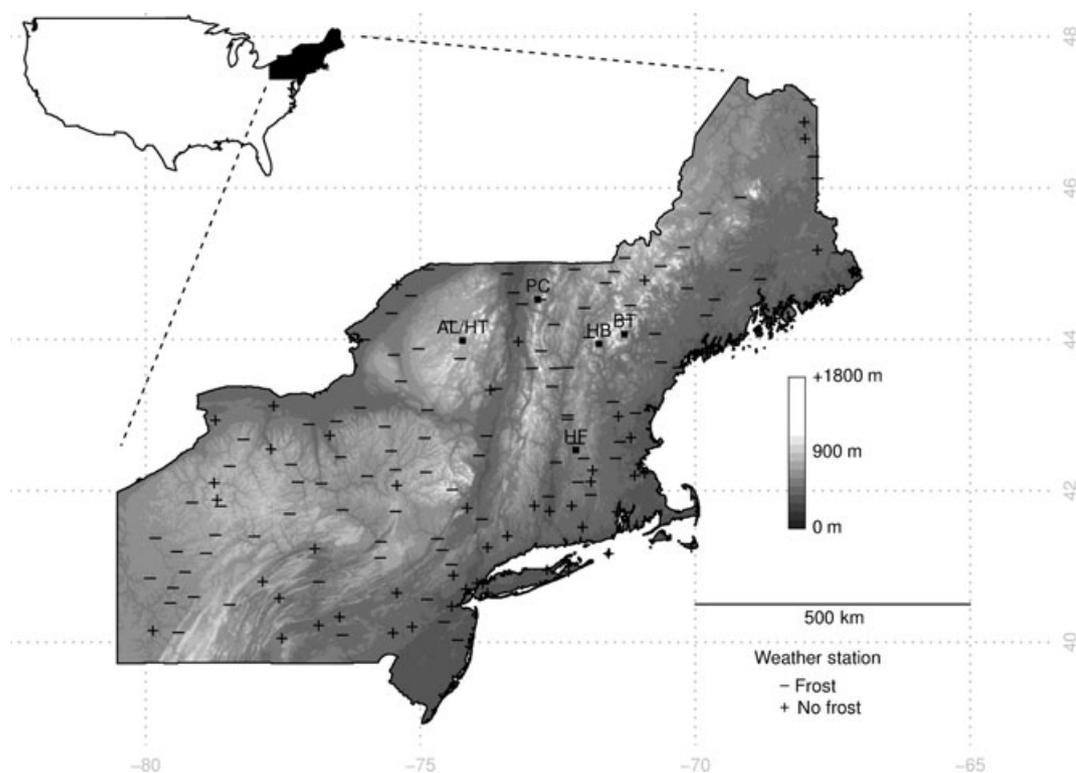
Fig. 2 Map of study region with inset showing location within the conterminous US. Locations of the 157 selected National Climatic Data Center weather stations are indicated with '+' or '−', depending on whether or not the site was affected by frost. Locations of near-surface remote sensing and field observation sites are indicated by solid boxes (■): Hubbard Brook Experimental (HB), Harvard Forest (HF), Proctor Maple Research Center (PC), Bartlett Forest (BT), Arbutus Lake and Huntington Forest (AL/HT). Topography is included as a grayscale in background.

Jersey, Connecticut, Rhode Island, Massachusetts, New Hampshire, and Maine (Fig. 2). Forest types within the study area are dominated by northern hardwood forest, with substantial areas of oak-hickory forest in the southern part of the study area. Topography in the study area ranges from sea level to 1917 m, and includes the Green Mountains, Adirondack Mountains, Taconic Mountains, the Alleghany Plateau, and the White Mountains.

Field observations of vegetation phenology were collected at two sites: (1) the Hubbard Brook Experimental Forest located in the White Mountain National Forest, New Hampshire; and (2) the Harvard Forest Long Term Ecological Research site in Massachusetts, located about 110 km west of Boston. The data sets and measurement protocols for each of these sites are described in Richardson *et al.* (2006), and specifics regarding data analysis are presented in Section 2.2.

Near-surface remote sensing data acquired by webcams were obtained from the PhenoCam image archive (Richardson *et al.*, 2009; Sonnentag *et al.*, 2012; www.hubbard-brook.org) for six deciduous forest sites within the study area: Hubbard Brook Experimental Forest (HB), Bartlett Experimental Forest (BF), Proctor Maple Research facility (PC), Harvard Forest LTER (HF), Arbutus Lake in Huntington Forest (AL), and Huntington Lodge at Huntington Forest (HT). The cameras at these sites all face north at an oblique (~20°) or near horizontal view angle, with fields-of-view dominated by mixtures of

hardwood species. Details related to the site characteristics for both the field observation sites as well as the near-surface remote sensing locations is provided in Table 1. A map showing the location of field observation and near-surface remote sensing sites is provided in Fig. 2. A detailed explanation of how the camera data were used is given in Section 2.5.

Field observations of phenology

At Hubbard Brook, canopy development observations for sugar maple, American beech, and yellow birch were made at nine locations along an elevation gradient ranging from 250 to 825 m asl. (stations HQ to 7T, Table 1, Richardson *et al.*, 2006, http://www.hubbardbrook.org). At each location, the canopy development status of three trees for each species has been recorded at weekly intervals during spring and fall since 1989. Leaf development stages are recorded using a spring phenology index that ranges from 0 (unexpanded buds) to 4 (summer canopy conditions, little sky visible through crowns). Following Richardson *et al.* (2006), we used index values of 1.5 (bud swelling/small leaves visible) and 3.5 (leaves 75% expanded, sky mostly obscured through crown) to define the timing of leaf emergence and mature canopy, respectively (see Table 2).

At Harvard Forest observations of leaf development for 33 different woody species are made at 3–7 day intervals from

Table 1 Characteristics of (1) phenology plots at Hubbard Brook Experimental Forest (HB) and Harvard Forest Long Term Ecological Research site (HF); and (2) near-surface remote sensing locations at the Proctor Maple Research Center (PC), Bartlett Experimental Forest (BT), the Arbutus Lake (AL) and Huntington Forest (HT) sites. We report elevation above sea level (asl), observation frequency for field observations of phenology and near-surface remotes sensing, and the aspect of the site and species composition. Both HB and HT near-surface remote sensing sites included regions-of-interest (ROI) that were at different elevation from the camera. The estimated elevation of the ROI in each case is reported between round brackets

Plot	Latitude/Longitude	Elev. (m asl)	Sampling frequency	Aspect	Dominant Species
HB Field observations:					
HQ	–	259	7 days	South	
5B	–	482	7 days	South	
1B	–	488	7 days	South	
4B	–	503	7 days	South	
7B	–	616	7 days	North	*Fagus grandifolia, Acer saccharum, Betula alleghaniensis*
4T	–	744	7 days	South	
5T	–	756	7 days	South	
6T	–	786	7 days	South	
7T	–	823	7 days	North	
HF	–	~340	3–7 days	/	
Near-surface remote sensing:					
HB	43.95°N/71.72°W	259 (550)	60 min	South	*Fagus grandifolia, Acer saccharum, Betula alleghaniensis*
BT	44.06° N/71.29° W	268	10 min (12–13 h)	South	*Acer sp., Fagus grandifolia*
PC	44.06° N/72.87° W	403	30 min	South	*Acer sp.*
HF	42.53 °N/72.19 °W	340	30 min	South	*Quercus rubra*
AL	43.98° N/72.23° W	535	60 min	South	*Fagus grandifolia, Acer saccharum, Betula alleghaniensis*
HT	43.97° N/74.22° W	500 (600)	30 min	South	*Fagus grandifolia, Acer saccharum, Betula alleghaniensis*

Table 2 Definitions for the spring 'phenology index' used by field observers at Hubbard Brook (after Richardson *et al.*, 2006)

Rating	Description
0	No change from winter conditions, unexpanded buds only
1	Bud swelling noticeable
2	Small leaves or flowers visible, initial stages of leaf expansion, leaves about 1cm long
3	Leaves 50% of final length, leaves obscure 50% of sky as seen through crowns
3.5	Leaves 75% expanded, sky mostly obscured through crown, crowns not yet in summer condition
4	Canopy appears in summer condition, leaves fully expanded, little sky visible through crowns

April through June (Richardson & O'Keefe, 2009, http://harvardforest.fas.harvard.edu). Data collection started in 1990 and is ongoing. Specific measurements include the percentage of buds that have burst (BB) and the percentage of leaves that have reached 75% (L75) and 95% (L95) of final leaf size. In this analysis, we use the day of the year on which 100% of observations have reached BB and L75 to identify the start and end of the leaf development period, respectively. For consistency with observations collected at Hubbard Brook, we only use observations of sugar maple, American beech, and yellow birch.

To provide a baseline for comparison against average climate conditions, we calculated the long term mean for each of the phenological indicators at both Harvard Forest and Hubbard Brook (1990–2009 and 1989–2009, respectively). Using the Hubbard Brook data, which includes data that span a significant gradient in elevation (Table 1), we used analysis of covariance (ANCOVA) to investigate whether slopes or intercepts of relationships between mean transition dates and

elevation differed significantly among species. We estimated two ANCOVA models. In the first model, we allowed the intercept, but not the slope, to vary with elevation. In the second model, we allowed both the intercept and the slope to vary with elevation. Model selection was based on the Akaike Information Criterion (Akaike, 1974), which calculates the Kullback–Leibler distance between model predictions and observations, with lower values indicating a better model fit. All reported regression coefficients and associated ANCOVA results for both 2010 and long-term measurement data are reported with significance levels of $P < 0.01$ unless indicated otherwise.

Near surface air temperatures and heat sum models

Air temperature data were obtained from the National Climatic Data Center (NCDC, http://www.ncdc.noaa.gov). The data set included measurements of daily minimum, maximum, and average air temperature ($T_{min}, T_{max}, \bar{T}$) from 157

stations located within the study area (Fig. 2), where at least 75% of daily values were available for 1971–2010. Temperature records of T_{min}, T_{max}, and $\bar{T}$ at the Hubbard Brook headquarters were downloaded from the Hubbard Brook Ecosystem Study data repository (http://www.hubbard-brook.org). To adjust these data for differences in elevation at each field site (see Table 1) we used a lapse rate of 0.6 °C/ 100 m (Richardson *et al.*, 2006).

To characterize the nature and magnitude of the 2010 late spring frost we used daily T_{min}, $\bar{T}$ and their associated anomalies relative to long-term averages (1971–2001) between DOY 1 and 170 for each station and field site. To convert the temperature data into units that are most relevant to spring leaf phenology in the region, we also computed daily values and anomalies in growing degree days (GDD) at each station (Cannell & Smith, 1983; Richardson *et al.*, 2006; Schwartz *et al.*, 2006). By convention, GDD is calculated by accumulating daily average temperatures above a prescribed base temperature for a specified period:

$$\text{GDD} = \sum_{i=\text{DOY}_1}^{\text{DOY}_2} ((\bar{T}_\tau - T_b) \text{ for } \bar{T}_\tau > T_b; 0 \text{ for } \bar{T}_\tau \leq T_b) \quad (1)$$

where T_b is the base temperature, DOY_1 to DOY_2 defines the period of interest, and $\bar{T}$ is the daily mean temperature. GDD was calculated for both the long-term average and 2010 average air temperatures using a base temperature of 4 °C following Richardson *et al.* (2006).

Eddy covariance and radiometric measurements

Eddy covariance measurements of carbon dioxide (CO_2), water vapor (H_2O), and sensible heat fluxes were acquired from the AmeriFlux site at Bartlett Experimental Forest. The net ecosystem CO_2 exchange was measured at 30-min intervals using an eddy covariance system. A quantum sensor mounted on the tower measured incident photosynthetically active radiation (PAR_D) above the canopy. Below-canopy transmitted PAR (PAR_T) was calculated as the average flux measured with six quantum sensors arranged in a circle (Ø 30 m) centered on the instrumentation tower. Complete details related to site characteristics at the Bartlett Forest AmeriFlux site are provided by Ollinger & Smith (2005), whereas tower instrumentation and data processing details are given by Jenkins *et al.* (2007).

To partition net ecosystem exchange (NEE) into gross ecosystem productivity (GEP) and ecosystem respiration (R_{eco}), we used a light response curve model following the approach used by Jenkins *et al.* (2007). We calculated daily sums of GEP (g C m^{-2} d^{-1}), excluding days when more than 25% of daytime NEE data were missing. To provide smooth gap-filled data, we computed three-day moving averages of the daily GEP values. Daily mean values for 2004–2009 were then used to estimate average GEP.

Downwelling and transmitted PAR measurements were used to estimate the effective leaf area index (LAI_e) based on the Beer–Lambert equation (Turner *et al.*, 2003; Monteith & Unsworth, 2007), where k is the canopy extinction coefficient when the solar zenith angle is ~57°, i.e. 1 radian (APPENDIX S1

Eq. 1a and b). Under these conditions, the leaf projection function (g, APPENDIX S1 Eq. 1c) converges to 0.5 (Warren Wilson, 1960; Nilson, 1971; Lang *et al.*, 1985). To estimate daily LAI_e, we averaged the morning and afternoon LAI_e values and residual outliers were removed using a 3 days moving average.

Near-surface remote sensing and GEP dynamics

Near-surface remote sensing images for 2006–2010 at the Bartlett Forest site and 2009–2010 at all other sites were acquired for each site (Table 1). For each camera, a region-of-interst (ROI) in the camera field-of-view was selected that provided a representative sample of forest vegetation in the surrounding landscape. To characterize canopy dynamics, we used the camera ROI data to compute an index called the green chromatic coordinate (*gcc*):

$$gcc = G/(R + G + B) \quad (2)$$

where R, G, and B are the average digital numbers from the red, green, and blue bands across all pixels in the ROI. The resulting time series were filtered using a 3-day moving window approach (Sonnentag *et al.*, 2012) and normalized to vary between 0 and 1. In addition, we calculated the daily rate of change in *gcc* for all years and sites to characterize the speed at which *gcc* changed at the start of the growing season.

Using a relationship between *gcc* and GEP based on data collected at the Bartlett Forest site, we estimated decreases in carbon uptake arising from frost damage at four of the Pheno-Cam sites in the study region where frost damage was clearly evident in *gcc* time series. We computed the 'carbon loss' (CL) as arising from two mechanisms: (1) direct losses arising from frost damage to leaf tissue (FD) and (2) indirect losses resulting from the photosynthetic opportunity cost to canopies caused by damaged leaves (OC). The total loss in carbon uptake is therefore the sum of carbon loss due to litterfall and reduced photosynthetic capacity:

$$CL = FD + OC \quad (3)$$

To estimate carbon loss due to FD, we first established a linear relationship between *gcc* and LAI_e (DOY 100–170) using data from Bartlett Forest. FD at each site was then estimated as a function of changes in LAI_e before and after the frost event, and transformed to units of carbon using the leaf mass per unit area (LMA):

$$FD = LAI_{DEC} \times LMA \quad (4)$$

where LAI_{DEC} is the decrease in LAI_e estimated from the change in *gcc*, and LMA is 70 g C m^{-2} (Cramer *et al.*, 2000).

To compute OC at each site, we use *gcc* time series as a proxy for GEP (Ahrends *et al.*, 2009; Migliavacca *et al.*, 2011). We estimated linear models that predict daily GEP as a function of daily *gcc* (DOY 100–170, years 2007–2009) using Bartlett Forest GEP and camera data, and modeled 2010 GEP was validated against measured 2010 GEP values. The loss in carbon uptake was calculated as the difference between modeled GEP for each near-surface remote sensing site (GEP^{site}) and the Bartlett Forest site (GEP^{Bartlett}) for 2010. The site to site variability in GEP due to differences in phenological development

were corrected by subtracting the GEP of each site (GEP^{site}) and the Bartlett Forest site (GEP^{Bartlett}) for the nonfrost affected reference year 2009. Daily differences were integrated over the period between the time of maximum *gcc* before the frost event (no damage, DOY$_{fe}$) and the time of maximum *gcc* after the frost event (mature canopy, DOY$_{mat}$):

$$OC = \sum_{i=DOY_{fe}}^{DOY_{mat}} (GEP_i^{site\ 2010} - GEP_i^{Bartlett\ 2010}) - \quad (5)$$
$$(GEP_i^{site\ 2009} - GEP_i^{Bartlett\ 2009})$$

If no reference data were available, the correction term was dropped from Eq. 5. We report total carbon loss as the percentage of average yearly GEP (2004–2010) measured at Bartlett Experimental Forest.

Satellite remote sensing

Remotely sensed data used in the study, covering the entire study region, included the MODIS land-cover dynamics (MCD12Q2) and land cover type (MCD12Q1) products (Friedl *et al.*, 2010; Ganguly *et al.*, 2010). The MODIS land-cover dynamics product provides estimates for the day-of-year on which key phenophase transitions occur in each 500-m MODIS pixel, based on enhanced vegetation index time series computed using nadir BRDF-Adjusted Reflectance (NBAR-EVI) data (Schaaf *et al.*, 2002; Zhang *et al.*, 2003, 2006). In this study, we use MODIS-derived estimates for the date of onset of greenness increase (G$_{in}$; i.e., roughly corresponding to the date of leaf emergence) and the date of onset of maximum greenness (G$_{max}$; i.e., roughly corresponding to the date on which the canopy reaches maximum leaf development). The MODIS land cover type product provides a classification at each 500-m MODIS pixel for the dominant land cover class, based on the International Geosphere-Biosphere Programme (IGBP) classification scheme. In addition, a 90-m spatial resolution digital elevation model based on the Shuttle Radar Topography Mission was acquired from the Consortium for Spatial Information website (http://www.cgiar-csi.org).

MODIS land-cover dynamics data were obtained for the period 2001–2010. Using these data, long-term (2001–2009) averages and standard deviations (*n* valid retrievals >4) were calculated for G$_{in}$ and G$_{max}$ for each 500-m cell in the study region. Using these data we devised a simple classification scheme to characterize how the unique combination of an anomalously warm spring and late spring frost event affected canopy dynamics and productivity in the study region. The classification identifies pixels with statistically significant early leaf development (measured by G$_{in}$) and delayed canopy maturation (measured by G$_{max}$). Specifically, pixels in 2010 for which G$_{in}$ or G$_{max}$ values deviated by one or two standard deviations from 2001 to 2009 averages were identified as having experienced mild and severe frost, respectively (F$_m$ and F$_s$; APPENDIX S1 Eq. 2a and b). Using the MODIS land cover type product, we limited the analysis to pixels classified as IGBP classes 4 or 5 (deciduous and mixed forests, respectively). The total area mapped as being affected by severe frost is reported and used to estimate regional GEP losses. Using the digital elevation model, we also examine patterns in G$_{in}$ and G$_{max}$, stratified by altitude.

Results

Anomalies in temperature and growing degree days

Surface air temperature measurements indicate that the winter and spring of 2010 in the study region were unusually warm with large positive anomalies in T$_{min}$ (Fig. 3). Late April and early May were characterized by anomalies and temperatures that frequently exceeded the GDD base temperature of 4 °C. As a result, GDD increased early in 2010 compared with long-term GDD values. The late spring frost is clearly evident in early May, when warm temperatures were abruptly interrupted by minimum temperatures well below freezing at 70% of the NCDC stations for the
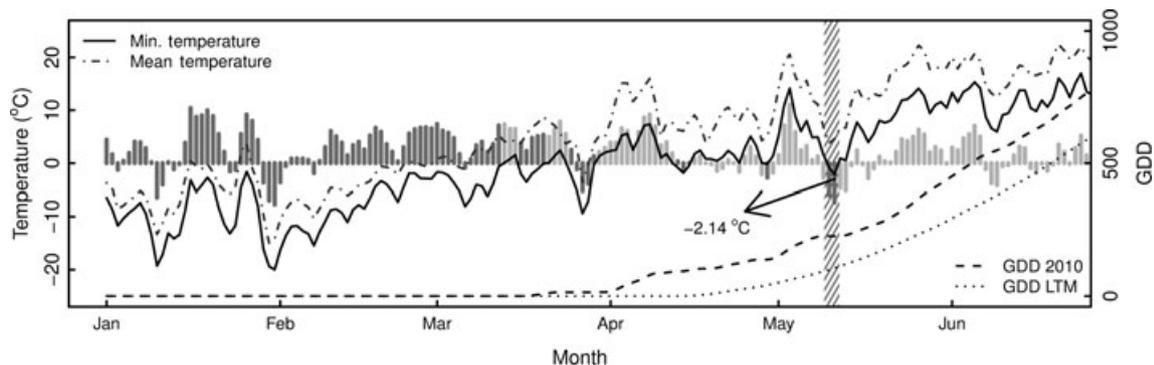

Fig. 3 Daily temperature patterns at frost affected sites in January–July 2010. The plot shows average daily mean and minimum temperatures. Anomalies in minimum temperature (relative to 1971–2000) are plotted as bars, where light gray bars represent anomalies with a minimum daily temperature above freezing and dark gray bars represent anomalies below freezing. The crosshatched box identifies the late spring frost (DOY of year 129 – 131). Dotted and dashed black lines at the bottom of the plot show daily growing degree days (GDD) for the long-term mean (LTM) and in 2010, respectively.

period between DOY 129 and 131. During this period average T_{min} was -2.1 ± 1.6 °C with a minimum of -12.8 °C or -7.3 °C below the climatological mean at frost-affected sites.

Phenological Indicators

Field observations. Field observations at the Hubbard Brook and Harvard Forest field sites showed dates for the start of the growing season that were 15, 14, and 13 days early for sugar maple, American beech, and yellow birch, respectively, compared with long-term averages (1994–2009). Specifically, ANCOVA results showed significantly different intercepts ($P < 0.001$, Fig. 4), but no significant differences in the slopes of regression models for the 2010 data compared with the long-term average (Fig. 4). These results indicate that the phenological response to warmer spring temperatures was uniform across elevations and that the relative timing in budburst as a function of altitude was not altered. The relationship between altitude and the timing of leaf out (hereafter referred to as the 'phenological lapse rate') was species-specific. More specifically, the timing of leaf emergence varied with elevation at a rate of 2.5, 2.8, and 4.1 days per 100 m for sugar maple, yellow

birch, and American beech, respectively. In other words, the timing of leaf emergence changed more rapidly with elevation in American beech than in sugar maple or yellow birch.

The timing of maximum canopy development at Harvard Forest and the Hubbard Brook headquarters was also early in 2010 relative to long-term average. At the Hubbard Brook headquarters maximum canopy development dates were 17, 11, and 13 days earlier than the long-term averages for sugar maple, American beech, and yellow birch, respectively. At Harvard Forest, sugar maple, American beech, and yellow birch reached maximum canopy development 13, 10, and 16 days early (respectively) relative to long-term averages. ANCOVA analysis of the relationship between the timing of maximum canopy development and elevation showed similar slopes (but different intercepts) for American beech and yellow birch ($P < 0.001$). The estimated slope and intercept for sugar maple in 2010 were both significantly different ($P < 0.05$) from long-term average values, suggesting that canopy development in sugar maples was delayed at higher altitudes. Indeed, the bottom panel of Fig. 4 shows that the timing of maximum canopy development for sugar maples at high elevation was similar to the long-term average.
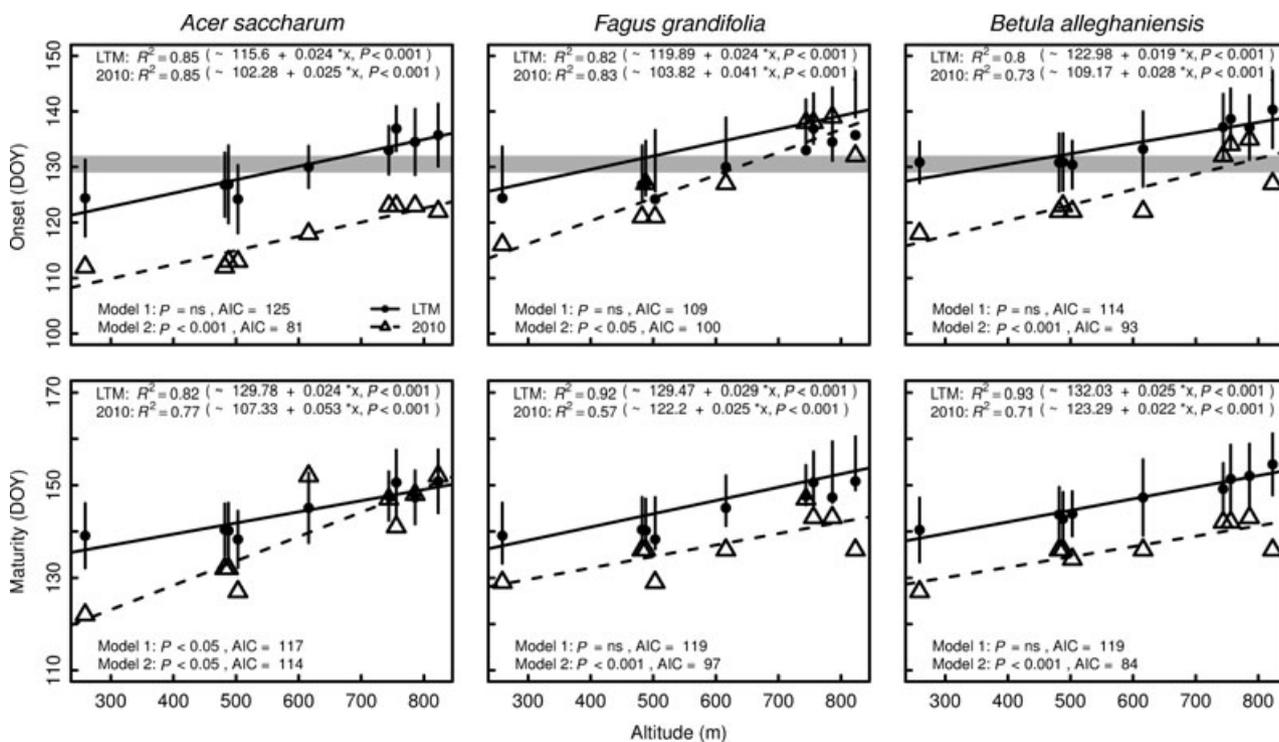

Fig. 4 Regression analysis showing the relationship between elevation and the timing of canopy development for sugar maple, American beech, and yellow birch at Hubbard Brook. The top panel plots DOY for the start of season against elevation; the bottom panel plots DOY for the timing of canopy maturity against elevation. Long-term mean (LTM) values are plotted with solid dots and black lines, with vertical lines at each point indicating ± 1 standard deviation. Data from 2010 are plotted using open triangles and dashed lines.

Phenological lapse rates for the timing of maximum canopy development in 2010 were 5.3, 2.2, and 2.5 days per 100 m for sugar maple, yellow birch, and American beech, respectively.

Near-surface remote sensing. Time series of *gcc* derived from webcams were used to assess differences in phenology across sites and across years (Fig. 5). The Bartlett Forest and Harvard Forest sites, which were not affected by frost, do not show any late spring decline in *gcc*. Data from Hubbard Brook, the Proctor Maple Research Center, and especially Arbutus Lake and Huntington, on the other hand, show pronounced declines in *gcc* immediately after the frost event. For comparison, the bottom panel of Fig. 5 shows that in 2009 *gcc* increased monotonically throughout the spring at all sites. The timing and rate of increase in *gcc* in 2010 is earlier and steeper compared with 2009, which

reflects early and rapid leaf unfolding in response to the anomalously warm spring. Indeed, the average rate of change in *gcc* more than doubled from $7\% \pm 2$ *gcc* day^{-1} in 2009 to $16\% \pm 5$ *gcc* day^{-1} in 2010.

Estimated potential loss in carbon gain

Figure 6 illustrates the strong linear relation between the *gcc* and LAI_e ($R^2 = 0.94$, $P < 0.001$) and between *gcc* and GEP ($R^2 = 0.84$, $P < 0.001$) at the Bartlett Forest site based on data from 2007 to 2009 for DOY 100–170. Maximum LAI_e at this site is about 4.2, which is representative of hardwood forests in the study region. More importantly, application of these regression parameters to *gcc* data from 2010 and corresponding LAI_e and GEP values show a strong linear relationship ($R^2 = 0.89$, $P < 0.001$ and $R^2 = 0.83$, $P < 0.001$ for LAI_e and GEP, respectively).
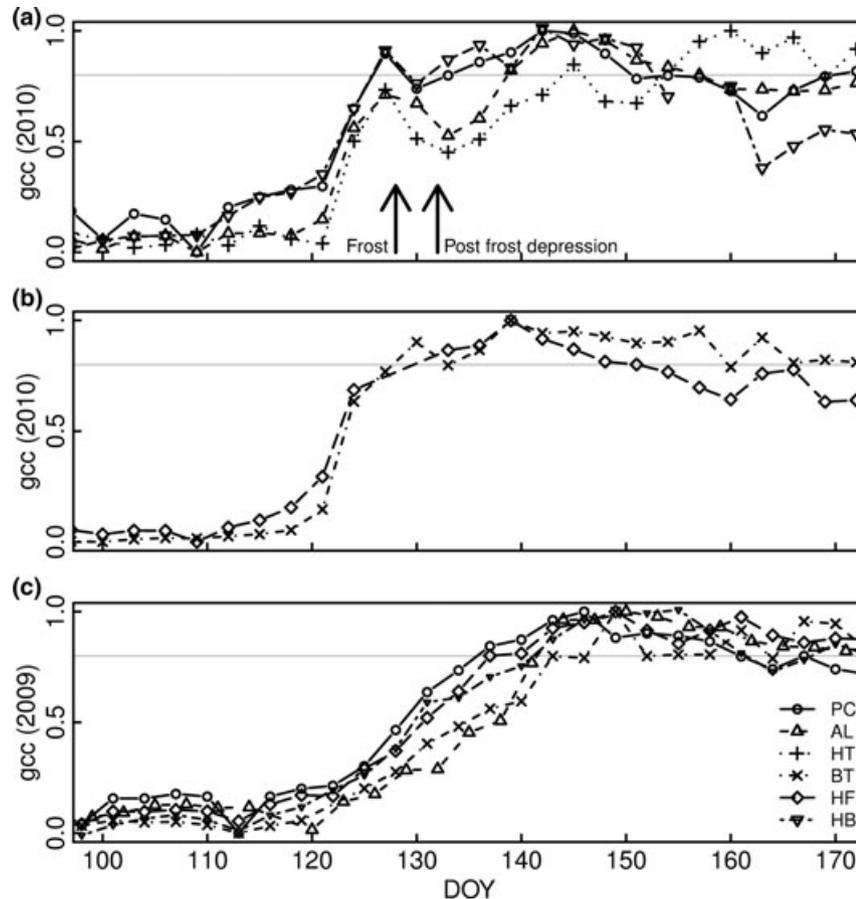

Fig. 5 Time series of the *gcc* during the spring of 2009 and 2010 (DOY 100–170) for six different near surface remote sensing sites located in the study region: Hubbard Brook (HB), Harvard Forest (HF), Proctor Maple Research Site (PC), Bartlett Forest (BT), Arbutus lake (AL), and Huntington National Forest (HT). The gray horizontal line at *gcc* = 0.8 provides a visual aid to assesses *gcc* progression and the recovery after the spring frost event. (a) locations affected by the late spring frost during the spring of 2010; (b) locations not affected by the late spring frost during the spring of 2010; (c) spring of 2009 reference time series for all sites (excluding HT because of missing data).
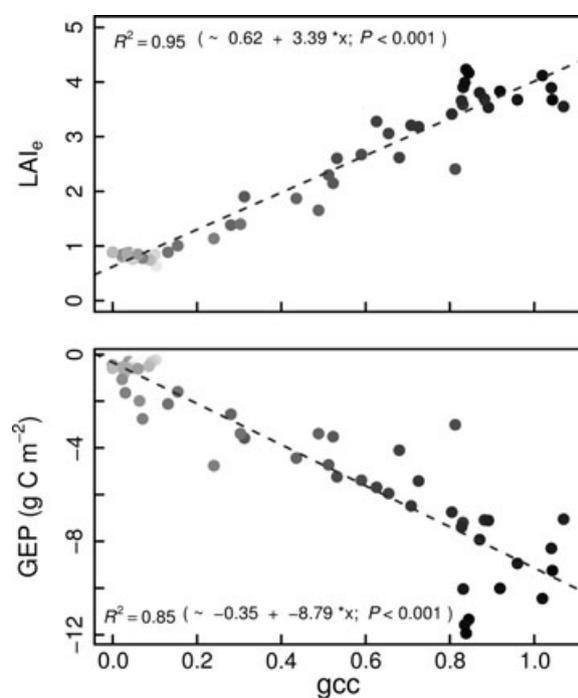
Fig. 6 Scatterplots of LAI_e (top panel) and daily GEP (bottom panel) against gcc at Bartlett Forest between DOY 100 (light gray) and 170 (dark gray) using data collected in 2007–2009. Linear regression models are shown as gray dashed lines.

Using these relationships, we estimate decreases in LAI_e of 14–33% relative to maximum LAI_e at each of the PhenoCam sites that were affected by frost (Fig. 5), which translates to carbon losses through leaf litterfall that range from 43 to 104 g C m^{-2} (Eq. 4). In contrast, changes in net carbon uptake inferred from gcc data (Eq. 5) are more variable, ranging from a low net loss at Arbutus Lake of 10 g C m^{-2} to a maximum of 49 g C m^{-2} for the Huntington Forest site. Estimates for total carbon loss (Eq. 3) due to the spring frost event ranged from 70 g C m^{-2} to 153 g C m^{-2}, or 7% to 14% of the average annual GEP at Bartlett Forest, based on data from 2004 to 2010 (1061 ± 82 g C m^{-2}). A summary of the results for each camera site is given in Table 3.

Regional assessment using satellite remote sensing

In the final part of our analysis we use data from the MODIS land-cover dynamics product to examine regional patterns in the response of forest canopy phenology to anomalous spring climate in 2010. Results from this analysis show that affected areas are clearly associated with higher elevation areas in the study region including the Green Mountains, Adirondack Mountains, Taconic Mountains, the Alleghany Plateau, and to a lesser extent the White Mountains (Fig. 7).

Table 4 presents data illustrating the relationship between elevation and areas in the study region that were identified from MODIS as affected by the frost event. Note that all three classes exhibited earlier onset of greenup (G_{in}) by roughly 2 weeks. The average elevation of 'mild' frost damage (F_m) was 539 ± 194 m asl; for severe frost events (F_s), the average elevation was 572 ± 157 m. The area affected by severe frost is shown in Fig. 7 and encompassed ~8753 km^2, which is equivalent to roughly 4% of the study area. Furthermore, consistent with field observations, MODIS data from 2010 data indicate that leaves emerged and reached maturity more rapidly at locations not affected by frost compared with locations that were affected by frost. Unaffected regions required 63 ± 20 days from G_{in} to G_{max}. Locations affected by mild and severe frost, on the other hand, exhibited green-up periods of up to 68 ± 15 and 74 ± 14 days. Corresponding long-term averages for this period are 48 ± 8 and 48 ± 7 days, respectively. Finally, combining the remotely sensed area affected by frost with predictions of carbon loss based on the relationships presented in Section 3.3, we estimate the carbon loss in forested areas identified from MODIS in the study area to range 614–1336 × 10^9 g C.

Table 3 Percentage decrease in excess green (gcc) and the associated loss of potential carbon gain (litterfall, photosynthesis) as a result of the late spring frost event calculated for Hubbard Brook Experimental Forest (HB), the Proctor Maple Research Center (PC), the Arbutus Lake (AL) and Huntington Forest (HF) national park sites. The percentage loss in annual GEP is reported relative to an average of 1060 ± 90 g C m^{-2} y^{-1} (2004–2009) based on measurements at Bartlett Experimental Forest

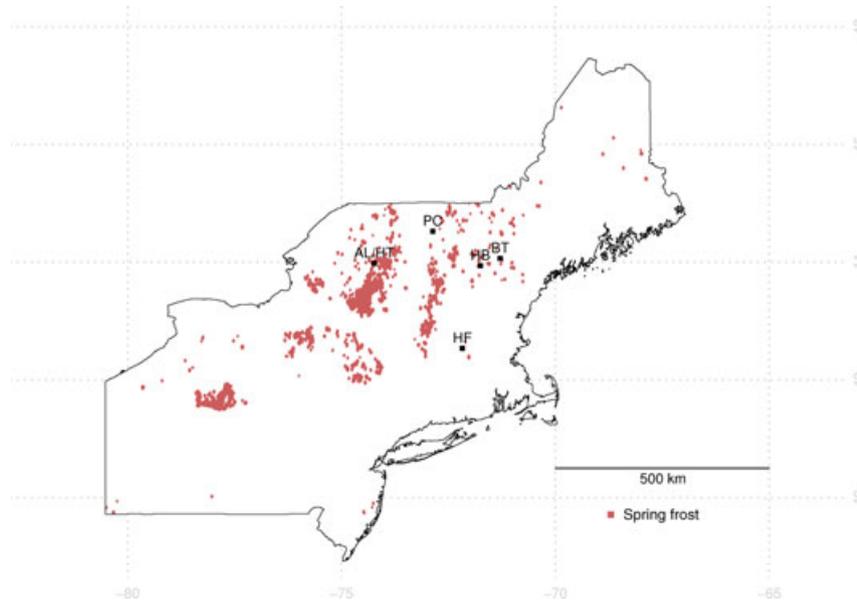| Site	gcc decrease (%)	Frost induced litterfall (g C m^{-2})	Lost potential carbon gain (g C m^{-2})	Total lost potential carbon gain (g C m^{-2})	Total lost potential carbon gain (% of annual GEP)
PC	16	52	26	78	7
HB	24	43	27	70	7
AL	14	75	10	85	8
HT	33	104	49	153	14

Fig. 7 A map showing locations classified as affected by severe frost and delayed canopy maturity, based on MODIS data. Superimposed upon this map are site locations for the field observations and near-surface remote sensing (■): Hubbard Brook (HB), Harvard Forest (HF), Proctor Maple Research Center (PC), Bartlett Forest (Bt), Arbutus Lake and Huntington National Forest (Al/HT).

Table 4 Summary statistics for samples of MODIS land-cover dynamics data in the region of interest with no, mild, or severe frost-related delay in canopy development. We report the mean ± one standard deviation for the average altitude, and the timing of greenness increase (G_{in}), greenness maximum (G_{max}), and greenup length ($G_{max} - G_{in}$) for both 2010 and the long-term mean (LTM)

	Greenness Increase		Greenness Maximum		Greenup Length		Altitude
	2010	LTM	2010	LTM	2010	LTM	(m asl)
No frost	96 ± 13	108 ± 8	160 ± 16	165 ± 10	63 ± 20	57 ± 16	301 ± 194
Mild frost	102 ± 11	117 ± 8	170 ± 11	165 ± 8	68 ± 15	48 ± 8	539 ± 194
Severe frost	101 ± 10	117 ± 8	174 ± 10	163 ± 8	73 ± 14	46 ± 7	573 ± 157

Discussion

In this study, we used the exceptionally warm spring and late spring frost event of 2010 in the northeastern United States to assess species-specific and regional responses of hardwood forests to this scenario. Our analysis focused on four main issues, which we discuss below.

Species-specific responses to frost at different elevations

Average and minimum daily air temperatures in the spring of 2010 were unusually warm across the northeastern US (Fig. 3). Consequently, leaves emerged earlier (up to 10–14 days early relative to long-term mean) and with more vigor than usual (Fig. 5). These results are consistent with a large body of previous research demonstrating the linkage between thermal forcing and spring phenology in deciduous tree species (Heide,

1993; Gansert *et al.*, 1999; Wesołowski & Rowiński, 2006). Phenological data collected at different elevations at Hubbard Brook showed phenological lapse rates (Δdays per 100m) for dominant tree species that were consistent with long-term means. Lapse rates for sugar maple and yellow birch both followed Hopkins law at ~2.4 ± 0.37 days per 100 m (Hopkins, 1938).

In addition to triggering early leaf development, anomalously warm spring temperatures increase the sensitivity of bud and leaf tissues to frost (Martin *et al.*, 2010). In 2010, near surface air temperature data in the northeastern US reveal a pronounced frost event throughout most of the region from May 9 to 11 (DOY 129–131, Fig. 2). While freezing temperatures were widespread throughout the region (average minimum temperature of −2.1 ± 1.6 °C), minimum temperatures at higher elevations in the region clearly exceeded the threshold required to produce sustained damage to leaf tissue (−3 °C, Sakai & Larcher, 1987). As a consequence,

frost damage resulted in extensive necrosis of healthy leaf tissue, especially at higher elevations, throughout the region. Our data show that sugar maples were most affected by frost damage, delaying canopy development, and doubling the phenological lapse rate for mature canopies in 2010 (5.3 days per 100 m) compared with the long-term mean (2.4 days per 100 m). These results suggest that sugar maple, an iconic and ecologically important tree in this region, may be particularly sensitive to changes in spring temperature regimes associated with climate change.

Species-specific responses arising from different growth strategies

Different species employ different growth strategies, and phenological responses vary among species depending on their sensitivity to different environmental forcing (e.g. temperature vs. photoperiod). Some species maximize resource acquisition by leafing out early, which increases both the growing season length and the risk of frost damage; others species are more conservative, but minimize the risk of freezing (Saxe et al., 2001). Differences in the rate of leaf unfolding can also influence sensitivity to frost events (Augspurger, 2009), and different species, organs, and life stages respond differently to extremes in spring temperatures (Sakai & Larcher, 1987; Augspurger, 2009). These factors highlight the inherent variability associated with how the phenology of different species respond to spring temperature forcing. Our results suggest that sugar maples tend to be opportunistic and leaf out early in the growing season, thereby maximizing carbon assimilation, but increasing the risk of frost damage (Norby et al., 2003). American beech and yellow birch, on the other hand, have more conservative growth strategies and leaf out later than sugar maple.

The exact mechanisms behind these differences remain unclear, and some have suggested that differences in specifies-specific phenology reflect differing evolutionary adaptations across successional stages (Hänninen & Tanino, 2011). For example, Borchert et al. (2005) concluded that the phenology of long-lived, late successional species is more strongly governed by photoperiod than temperature. This explanation is not consistent with the results from this study. Specifically, sugar maple is a dominant late successional species in temperate hardwood forests of the northeastern United States. However, as we describe above, in 2010 sugar maples were significantly more sensitive to spring temperature anomalies than American beech or yellow birch. As a consequence, leaf necrosis and delayed canopy development resulted in a net decrease in carbon assimilation by sugar maples. Although some of this

decrease can be compensated through activation of dormant or adventitious buds (Neilson & Wullstein, 1983), several studies indicate that recovery of tree canopies from spring frost damage is often incomplete relative to normal conditions (Gansert et al., 1999; Awaya et al., 2009).

Frost-induced changes in gross ecosystem productivity

At locations that were severely frost damaged, our results suggest that net carbon uptake decreased by 70–153 g C m^{-2} as a result of the 2010 frost event, which corresponds to 7–14% of annual GEP. It is important to note that this result depends on our assumption that GEP dynamics at Bartlett Forest is representative of temperate hardwood forests throughout the region. However, our estimates are consistent with other studies that relate the seasonality of canopy development to intra and interannual dynamics in GEP. For example, Richardson et al. (2009, 2010) estimate that a one-day shift in the timing of leaf emergence in temperate hardwood forests changes GEP by 5–10 g C m^{-2} yr^{-1}. Similarly, Urbanski et al. (2007) estimate that interannual variability at Harvard Forest is ~170 C m^{-2} yr^{-1}. Thus, our estimate of frost-induced loss in GEP ranges from 41% to 90% of the interannual variability in GEP.

At the regional scale, our analysis using satellite remote sensing data confirm that frost damage was widespread. Specifically, severely affected regions were concentrated in mountainous areas (Fig. 7) and encompassed roughly 8753 km^2. Upscaling our site-based estimate of GEP losses to this scale, we estimate the regional 'carbon cost' of the frost event to be between 614×10^9 g C and 1336×10^9 g C. Although recent studies have shown that medium resolution remote sensing data are able to capture detailed phenological dynamics in mountainous areas (Busetto et al., 2010; Guyon et al., 2011), we noted substantial variability in the relationship between altitude and the phenological response of forests that were captured by MODIS (Table 4). One obvious explanation for this variability is that frost damage depends quite heavily on site-specific conditions including local temperature inversions, cold air drainage in valleys (Fisher et al., 2006; Inouye, 2008), and topographically induced patterns in microclimate that fall below the 500 m spatial resolution of MODIS data.

Potential long-term impacts on community ecology

Disturbances, both natural and anthropogenic, influence the composition, structure, and function of forests (Dale et al., 2001), and it is now widely recognized that climate change is altering disturbance regimes in many

parts of the world. The results from this study suggest that changes in spring temperatures may have significant implications for community composition in higher elevation hardwood forests of the northeastern United States. Recent evidence suggests that warming temperatures are decreasing the range margin of sugar maple at higher elevations in favor of beech and birch (Beckage *et al.*, 2008). High altitude vegetation is already limited by topography, soils, and climate. An important implication of this work is that additional stress caused by more frequent spring frost events may lead to changes in community structure and sugar maple abundance at the species range margin. Our results therefore suggest that late spring frosts may provide a competitive advantage for yellow birch and American beech, at the expense of sugar maple.

As a consequence, warmer spring temperatures and increased frequency of spring frosts after leaf-out arising from climate change will not only affect short-term carbon budgets but also have the potential to alter forest composition, ecosystem function, and long-term biosphere-atmosphere interactions. McMahon *et al.* (2011) stress the importance of better representation of phenology and plant functional types in species distribution models. The results from this work, both support this contention and illustrate the need for more studies focused on extreme events to constrain and validate coupled climate, ecosystem, and species distribution models.

References

Ahrends HE, Etzold S, Kutsch WL *et al.* (2009) Tree phenology and carbon dioxide fluxes: use of digital photography for process-based interpretation at the ecosystem scale. *Climate Research*, **39**, 261–274.

Akaike H (1974) A new look at the statistical model identification. *Automatic Control, IEEE Transactions on*, **19**, 716–723.

Augspurger CK (2009) Spring 2007 warmth and frost: phenology, damage and refoliation in a temperate deciduous forest. *Functional Ecology*, **23**, 1031–1039.

Awaya Y, Tanaka K, Kodani E, Nishizono T (2009) Responses of a beech (*Fagus crenata Blume*) stand to late spring frost damage in Morioka, Japan. *Forest Ecology and Management*, **257**, 2359–2369.

Beckage B, Osborne B, Gavin DG, Pucko C, Siccama T, Perkins T (2008) A rapid upward shift of a forest ecotone during 40 years of warming in the Green Mountains of Vermont. *Proceedings of the National Academy of Sciences of the United States of America*, **105**, 4197–4202.

Blunden J, Arndt DS, Baringer MO (2011) State of the Climate in 2010. *Bulletin of the American Meteorological Society*, **92**, 1–266.

Borchert R, Robertson K, Schwartz MD, Williams-Linera G (2005) Phenology of temperate trees in tropical climates. *International Journal of Biometeorology*, **50**, 57–65.

Busetto L, Colombo R, Migliavacca M *et al.* (2010) Remote sensing of larch phenological cycle and analysis of relationships with climate in the Alpine region. *Global Change Biology*, **16**, 2504–2517.

Cannell M, Smith R (1983) Thermal time, chill days and prediction of budburst in *Picea sitchensis*. *Journal of Applied Ecology*, **20**, 951–963.

Chuine I (2010) Why does phenology drive species distribution? *Philosophical Transactions of the Royal Society of London. Series B, Biological Sciences*, **365**, 3149–3160.

Cramer J, Fahey T, Battles J (2000) Patterns of leaf mass, area and nitrogen in young Northern Hardwood forests. *American Midland Naturalist*, **144**, 253–264.

Dale VH, Joyce LA, McNulty S *et al.* (2001) Climate change and forest disturbances. *BioScience*, **51**, 723–734.

Dragoni D, Schmid HP, Wayson C, Potter H, Grimmond CSB, Randolph JC (2011) Evidence of increased net ecosystem productivity associated with a longer vegetated season in a deciduous forest in south-central Indiana, USA. *Global Change Biology*, **17**, 886–897.

Fisher JI, Mustard JF, Vadeboncoeur MA (2006) Green leaf phenology at Landsat resolution: scaling from the field to the satellite. *Remote Sensing of Environment*, **100**, 265–279.

Fitzjarrald DR, Acevedo O (2001) Climatic consequences of leaf presence in the eastern United States. *Journal of Climate*, **14**, 598–614.

Foster R (1992) Land-use history (1730–1990) and vegetation in central New England, USA. *Journal of Ecology*, **80**, 753–771.

Friedl MA, Sulla-Menashe D, Tan B, Schneider A, Ramankutty N, Sibley A, Huang XM (2010) MODIS Collection 5 global land cover: algorithm refinements and characterization of new datasets. *Remote Sensing of Environment*, **114**, 168–182.

Ganguly S, Friedl M, Tan B, Zhang X, Verma M (2010) Land surface phenology from MODIS: characterization of the collection 5 global land cover dynamics product. *Remote Sensing of Environment*, **114**, 1805–1816.

Gansert D, Backes K, Kakubari Y (1999) Altitudinal and seasonal variation of frost resistance of *Fagus crenata* and *Betula ermanii* along the Pacific slope of Mt. Fuji, Japan. *Journal of Ecology*, **87**, 382–390.

Gu L, Hanson PJ, Post WM *et al.* (2008) The 2007 Eastern US spring freeze: increased cold damage in a warming world. *BioScience*, **58**, 253–262.

Guirguis K, Gershunov A, Schwartz R, Bennett S (2011) Recent warm and cold daily winter temperature extremes in the Northern Hemisphere. *Geophysical Research Letters*, **38**, 2–7.

Guyon D, Guillot M, Vitasse Y, Cardot H, Hagolle O, Delzon S, Wigneron J-P (2011) Monitoring elevation variations in leaf phenology of deciduous broadleaf forests from SPOT/VEGETATION time-series. *Remote Sensing of Environment*, **115**, 615–627.

Hänninen H, Tanino K (2011) Tree seasonality in a warming climate. *Trends in Plant Science*, **16**, 412–416.

Heide OM (1993) Daylength and thermal time responses of budburst during dormancy release in some northern deciduous trees. *Physiologia Plantarum*, **88**, 531–540.

Hickling R, Roy DB, Hill JK, Fox R, Thomas CD (2006) The distributions of a wide range of taxonomic groups are expanding polewards. *Global Change Biology*, **12**, 450–455.

Hollinger DY, Goltz SM, Davidson EA, Lee JT, Tu K, Valentine HT (1999) Seasonal patterns and environmental control of carbon dioxide and water vapour exchange in an ecotonal boreal forest. *Global Change Biology*, **5**, 891–902.

Hopkins AD (1938) *Bioclimatics – A Science of Life and Climate Relations*. US Department of Agriculture, Washington.

Inouye D (2008) Effects of climate change on phenology, frost damage, and floral abundance of montane wildflowers. *Ecology*, **89**, 353–362.

Iverson LR, Prasad AM (1998) Predicting abundance of 80 tree species following climate change in the Eastern United States. *Ecological Monographs*, **68**, 465–485.

Jenkins JP, Richardson AD, Braswell BH, Ollinger SV, Hollinger DY, Smith ML (2007) Refining light-use efficiency calculations for a deciduous forest canopy using simultaneous tower-based carbon flux and radiometric measurements. *Agricultural and Forest Meteorology*, **143**, 64–79.

Jeong S-J, Ho C-H, Gim H-J, Brown ME (2011) Phenology shifts at start vs. end of growing season in temperate vegetation over the Northern Hemisphere for the period 1982–2008. *Global Change Biology*, **17**, 2385–2399.

Kelly AE, Goulden ML (2008) Rapid shifts in plant distribution with recent climate change. *Proceedings of the National Academy of Sciences*, **105**, 11823–11826.

Lang ARG, Yueqin X, Norman JM (1985) Crop structure and the penetration of direct sunlight. *Agricultural and Forest Meteorology*, **35**, 83–101.

Lenoir J, Gégout JC, Marquet P, de Ruffray P, Brisse H (2008) A significant upward shift in plant species optimum elevation during the 20th century. *Science*, **320**, 1768–1771.

Levis S, Bonan GB (2004) Simulating springtime temperature patterns in the community atmosphere model coupled to the community land model using prognostic leaf area. *Journal of Climate*, **17**, 4531–4540.

Marino GP, Kaiser DP, Gu L, Ricciuto DM (2011) Reconstruction of false spring occurrences over the southeastern United States, 1901–2007: an increasing risk of spring freeze damage? *Environmental Research Letters*, **6**, 024015–024023.

Martin M, Gavazov K, Körner C, Hättenschwiler S, Rixen C (2010) Reduced early growing season freezing resistance in alpine treeline plants under elevated atmospheric CO_2. *Global Change Biology*, **16**, 1057–1070.

McMahon SM, Harrison SP, Armbruster WS et al. (2011) Improving assessment and modelling of climate change impacts on global terrestrial biodiversity. *Trends in Ecology & Evolution*, **26**, 249–259.

Meehl GA, Karl T, Easterling DR et al. (2000) An introduction to trends in extreme weather and climate events: observations, socioeconomic impacts, terrestrial ecological impacts, and model projections. *Bulletin-American Meteorological Society*, **81**, 413–416.

Migliavacca M, Galvagno M, Cremonese E, Rossini et al. (2011) Using digital repeat photography and eddy covariance data to model grassland phenology and photosynthetic CO_2 uptake. *Agricultural and Forest Meteorology*, **151**, 1325–1337.

Monteith J, Unsworth M (2007) *Principles of Environmental Physics* (3rd edn). Academic Press, Burlington, MA.

Morin X, Viner D, Chuine I (2008) Tree species range shifts at a continental scale: new predictive insights from a process-based model. *Journal of Ecology*, **78**, 4–794.

Neilson RP, Wullstein LH (1983) Biogeography of two southwest American oaks in relation to atmospheric dynamics. *Journal of Biogeography*, **10**, 275–297.

Nilson T (1971) A theoretical analysis of the frequency of gaps in plant stands. *Agricultural Meteorology*, **8**, 25–38.

Norby RJ, Hartz-Rubin JS, Verbrugge MJ (2003) Phenological responses in maple to experimental atmospheric warming and CO_2 enrichment. *Global Change Biology*, **9**, 1792–1801.

Ollinger SV, Smith M-L (2005) Net Primary Production and canopy nitrogen in a temperate forest landscape: an analysis using imaging spectroscopy, modeling and field data. *Ecosystems*, **8**, 760–778.

Parmesan C, Yohe G (2003) A globally coherent fingerprint of climate change impacts across natural systems. *Nature*, **421**, 37–42.

Piao S, Friedlingstein P, Ciais P, Peylin P, Zhu B, Reichstein M (2009) Footprint of temperature changes in the temperate and boreal forest carbon balance. *Geophysical Research Letters*, **36**, 1–5.

Richardson AD, O'Keefe J (2009) Phenological differences between understory and overstory: a case study using the long-term Harvard Forest records. In: *Phenology of Ecosystem Processes* (ed. Noormets A), pp. 87–117. Springer, New York, NY, USA.

Richardson AD, Bailey AS, Denny EG, Martin CW, O'Keefe J (2006) Phenology of a northern hardwood forest canopy. *Global Change Biology*, **12**, 1174–1188.

Richardson AD, Braswell BH, Hollinger DY, Jenkins JP, Ollinger SV (2009) Near-surface remote sensing of spatial and temporal variation in canopy phenology. *Ecological Applications: A Publication of the Ecological Society of America*, **19**, 1417–1428.

Richardson AD, Black TA, Ciais P et al. (2010) Influence of spring and autumn phenological transitions on forest ecosystem productivity. *Philosophical Transactions of the Royal Society of London. Series B, Biological Sciences*, **365**, 3227–3246.

Sakai A, Larcher W (1987) *Frost Survival of Plants. Responses and Adaptation to Freezing Stress*. Springer-Verlag, Berlin, Germany.

Sakai RK, Fitzjarrald DR, Moore KE (1997) Detecting leaf area and surface resistance during transition seasons. *Agricultural and Forest Meteorology*, **84**, 273–284.

Saxe H, Cannell MGR, Johnsen Ø, Ryan MG, Vourlitis G (2001) Tree and forest functioning in response to global warming. *New Phytologist*, **149**, 369–399.

Schaaf CB, Gao F, Strahler AH, Lucht W, Li X et al. (2002) First operational BRDF, albedo nadir reflectance products from MODIS. *Remote Sensing of Environment*, **83**, 135–148.

Schwartz MD, Ahas R, Aasa A (2006) Onset of spring starting earlier across the Northern Hemisphere. *Global Change Biology*, **12**, 343–351.

Solomon S, Qin D, Manning M et al. eds (2007) *Climate Change 2007: The Physical Science Basis*, Cambridge University Press, New York, NY, USA.

Sonnentag O, Hufkens K, Teshera-Sterne C et al. (2012) Digital repeat photography for phenological research in forest ecosystems. *Agricultural and Forest Meteorology*, **152**, 159–177.

Turner DP, Ritts WD, Cohen WB et al. (2003) Scaling Gross Primary Production (GPP) over boreal and deciduous forest landscapes in support of MODIS GPP product validation. *Remote Sensing of Environment*, **88**, 256–270.

Urbanski S, Barford C, Wofsy S et al. (2007) Factors controlling CO_2 exchange on timescales from hourly to decadal at Harvard Forest. *Journal of Geophysical Research*, **112**, 1–25.

Warren Wilson J (1960) Inclined point quadrats. *New Phytologist*, **59**, 1–8.

Wesołowski T, Rowiński P (2006) Timing of bud burst and tree-leaf development in a multispecies temperate forest. *Forest Ecology and Management*, **237**, 387–393.

Zhang X, Friedl MA, Schaaf CB et al. (2003) Monitoring vegetation phenology using MODIS. *Remote Sensing of Environment*, **84**, 471–475.

Zhang X, Friedl MA, Schaaf CB (2006) Global vegetation phenology from Moderate Resolution Imaging Spectroradiometer (MODIS): evaluation of global patterns and comparison with *in situ* measurements. *Journal of Geophysical Research*, **111**, 1–14.

Supporting Information

Additional Supporting Information may be found in the online version of this article:

Appendix S1. Detailed formulas outlining: 1a-c The calculation of the effective leaf area index (LAIe) from incident photosynthetically active radiation (PAR) and 2a,b the classification rules as used to define mild and severe frost events (Fm and Fs, respectively) based upon Moderate Resolution Imaging Spectroradiometer (MODIS) land-cover dynamics product (MCD12Q2).

Please note: Wiley-Blackwell are not responsible for the content or functionality of any supporting materials supplied by the authors. Any queries (other than missing material) should be directed to the corresponding author for the article.